Large vacuum Rabi splitting in ZnO-based hybrid microcavities observed at room temperature

Jun-Rong Chen, Tien-Chang Lu, Yung-Chi Wu, Shiang-Chi Lin, Wei-Rein Liu, Wen-Feng Hsieh, Chien-Cheng Kuo, and Cheng-Chung Lee

Large vacuum Rabi splitting in ZnO-based hybrid microcavities observed at room temperature

Jun-Rong Chen,[1] Tien-Chang Lu,[1,a)] Yung-Chi Wu,[1] Shiang-Chi Lin,[1] Wei-Rein Liu,[1] Wen-Feng Hsieh,[1] Chien-Cheng Kuo,[2] and Cheng-Chung Lee[3]

[1]*Department of Photonics & Institute of Electro-Optical Engineering, National Chiao Tung University, Hsinchu 300, Taiwan*
[2]*Thin Film Technology Center, National Central University, Jhongli 320, Taiwan*
[3]*Department of Optics and Photonics, National Central University, Jhongli 320, Taiwan*

Wide-band gap ZnO semiconductors are attractive materials for the investigation of microcavity exciton polaritons due to the large exciton binding energy and oscillator strength. We report the growth and characterization of bulk ZnO-based hybrid microcavity. The phenomenon of strong exciton-photon coupling at room temperature has been observed in the ZnO-based hybrid microcavity structure, which consists of 30 pair epitaxially grown AlN/AlGaN distributed Bragg reflector (DBR) on the bottom side of the $3/2\lambda$ thick ZnO cavity and 9 pair SiO_2/HfO_2 DBR as the top mirror. The cavity quality factor is about 221. The experimental results show good agreement with theoretically calculated exciton-polariton dispersion curves based on transfer matrix method. From the theoretical and experimental exciton-polariton dispersion curves with two different cavity-exciton detuning values, the large vacuum Rabi splitting is estimated to be about 58 meV in the ZnO-based hybrid microcavity. © *2009 American Institute of Physics.*
[DOI: 10.1063/1.3079398]

Strong light-matter coupling in semiconductor microcavities (MCs) has attracted much attention since the pioneering work of Weisbuch *et al.*[1] in 1992. In MC structure with strong interaction of excitons and photons, the new quasiparticles termed cavity polaritons are created and characterized by bosonic properties including very light mass and controllable dispersions. These unique MC polariton properties provide the possibility to investigate the fundamental physical phenomena including strong light-matter interaction,[2,3] solid-state cavity quantum electrodynamics,[4] and dynamical Bose–Einstein condensates.[5,6] Besides, further applications of MC polaritons include polariton lasers,[7] polariton light-emitting diodes,[8] and polariton parametric amplifiers.[9] As far as material issues are concerned, GaAs-based MC structures have nearly lattice-matched AlGaAs/AlGaAs distributed Bragg reflectors (DBRs) and high-quality GaAs/AlGaAs quantum wells. Therefore, it is relatively easy to obtain high-quality-factor MCs. However, the strong-coupling phenomenon in GaAs-based MCs is hardly observed at room temperature (RT) due to the small exciton binding energy of about 4 meV for bulk GaAs materials.[10] In GaN-based semiconductors, the large exciton binding energy is about 26 meV for bulk GaN layers[11] and about 40–50 meV for quantum-well structures.[12] Consequently, the strong-coupling phenomenon,[2,3] polariton condensation,[6] and polariton laser[7,12] have been observed at RT from GaN-based MCs. Furthermore, ZnO-based MC is an attractive alternative for the study of polariton-related properties at RT since the exciton binding energy is as even larger about 60 meV for bulk ZnO layers. Although the ZnO material has been reported to be the mostly adapted for the realization of RT polariton lasers,[10] the related literature re-

porting the observation of cavity polaritons in ZnO-based MCs is relatively few.[13]

In this study, we report the epitaxial growth and optical characterization of bulk ZnO-based hybrid MCs. Strong coupling between the exciton and cavity modes was observed at RT according to the angle-resolved reflectivity and photoluminescence (PL) spectra. Theoretical analysis of the strong coupling was also performed by employing transfer matrix method to calculate the reflectivity spectra of the hybrid ZnO MCs.

The microcavity structure consists of a bulk ZnO $3/2\lambda$ thick cavity sandwiched between a bottom 30-pair AlN/AlGaN DBR and a top nine-period dielectric SiO_2/HfO_2 DBR. Here we chose λ to be 380 nm in air. The aluminum composition in the DBR was about 23% from the measurement of high-resolution x-ray diffraction. The AlN/AlGaN DBR was grown on (0001)-oriented sapphire substrates in a low-pressure high-speed rotating-disk metalorganic chemical vapor deposition system. During the growth, trimethylgallium and trimethylaluminum were used as group III source materials and ammonia (NH_3) as the group V source material. After thermal cleaning of the substrate in hydrogen ambient for 5 min at 1100 °C, a 30-nm-thick GaN nucleation layer was grown at 500 °C. The growth temperature was raised up to 1020 °C for the growth of 2.8 μm GaN buffer layer. Then, the AlN/AlGaN DBRs were grown under the fixed chamber pressure of 100 Torr similar to the previous reported growth conditions.[14] The bulk ZnO $3/2\lambda$ thick cavity was grown on AlN/AlGaN DBR by plasma-assisted molecular beam epitaxy system under the growth temperature of about 550 °C. The nine-period SiO_2/HfO_2 dielectric DBR was deposited by dual electron-beam gun evaporation system to complete the microcavity structure. The schematic sketch of the ZnO-based microcavity structure is shown in Fig. 1(a). The interface between the AlN/AlGaN DBR and the ZnO

---

a)Author to whom correspondence should be addressed. Electronic mail: timtclu@mail.nctu.edu.tw.
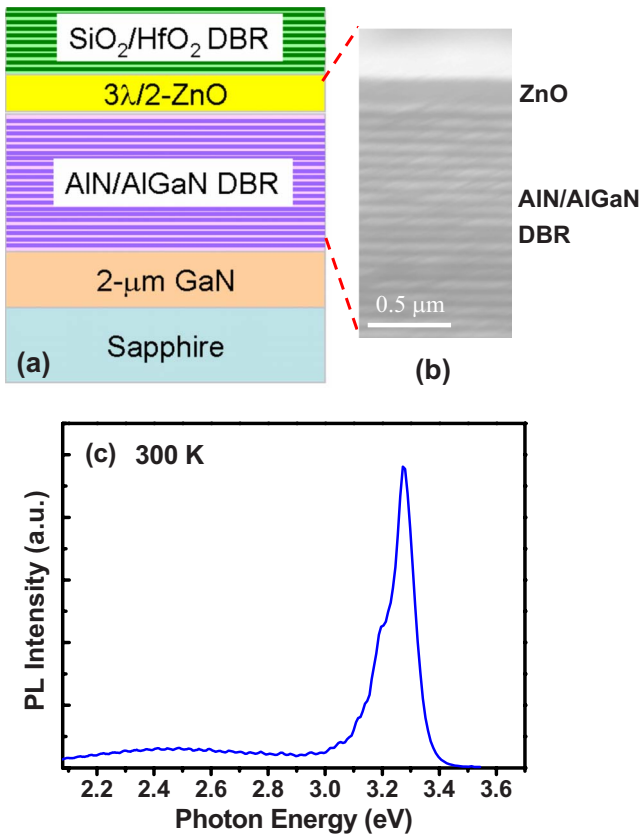
FIG. 1. (Color online) (a) The schematic diagram of the ZnO-based hybrid microcavity. (b) The cross-section image of the ZnO microcavity with bottom DBRs observed by SEM. (c) RT PL spectrum from the half-cavity ZnO film grown on AlN/AlGaN DBRs.

cavity is smooth as seen from the cross-sectional scanning electron microscope (SEM) image in Fig. 1(b). Figure 1(c) shows the RT PL spectrum from the ZnO film grown on AlN/AlGaN DBR. The good material quality of the ZnO film can be observed from the suppression of the deep level emission band in the RT PL spectrum.

The reflectivity spectra of a 30-pair AlN/$Al_{0.23}Ga_{0.77}$N DBR and a nine-pair SiO_2/HfO_2 DBR were measured at RT, respectively, for normal incidence, as shown in Fig. 2(a). The peak reflectivity of bottom AlN/AlGaN DBR is about 93% and the stop band width is about 145 meV. As for the top SiO_2/HfO_2 DBR, the peak reflectivity and the stop band width are 97% and 790 meV, respectively. The RT PL spectrum from a half-cavity structure (i.e., without the top SiO_2/HfO_2 DBR) is also shown in Fig. 2(a). It is found that the PL spectrum from the half-cavity ZnO layer is mostly
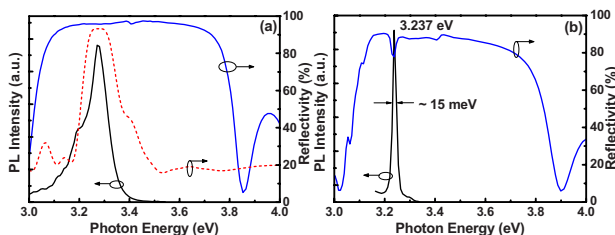

FIG. 2. (Color online) (a) The RT reflectivity spectra of a 30-pair AlN/$Al_{0.23}Ga_{0.77}$N DBR (dashed line) and a nine-pair SiO_2/HfO_2 DBR (solid line). RT PL spectrum from a half cavity is located within the stop band of the bottom and top DBRs. (b) RT reflectivity and PL spectra from the full hybrid microcavity.
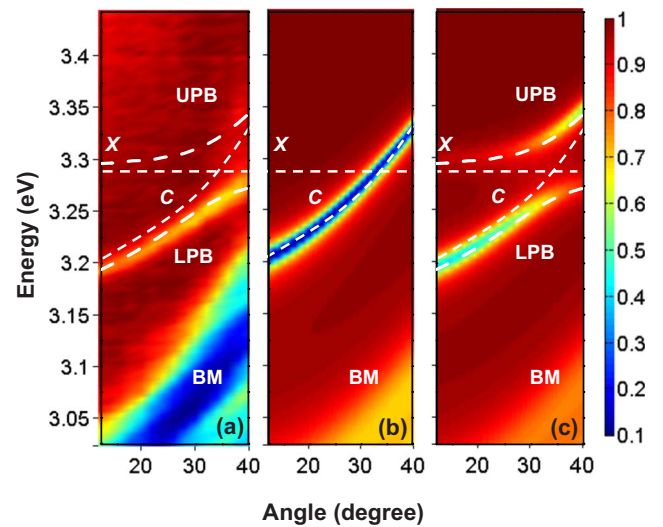

FIG. 3. (Color online) (a) The color map of the measured angle-solved reflectivity spectra from 10° to 40° at RT. (b) The color map of the calculated angle-solved reflectivity spectra from 10° to 40° without taking the resonant exciton into account. (c) The color map of the calculated angle-solved reflectivity spectra from 10° to 40° with taking the resonant exciton into account.

covered by the stop band width of the bottom and top DBRs. Figure 2(b) shows the RT reflectivity and PL spectra from the full ZnO MC structure at normal incidence. The PL linewidth is decreased to be about 15 meV ($\Delta\lambda \sim 1.73$ nm) due to the microcavity effect, and the PL peak energy is about 3.237 eV ($\lambda \sim 383$ nm). Therefore, the cavity quality factor $Q(=\lambda/\Delta\lambda)$ is about 221 when the pump spot size is about 3 μm. Furthermore, the cavity dip can be clearly observed in the reflectivity spectrum, which shows a precise alignment between the DBR stop band and the ZnO cavity thickness. We found that the cavity dip was strongly dependent on the sample position due to the thickness nonuniformity in the ZnO cavity layer and the bottom DBR.

RT angle-resolved reflectivity measurements were performed by using a two arm goniometer and a xenon lamp was employed as a white light source. The color map of the angular dispersion of measured reflectivity spectra from 10° to 40° is shown in Fig. 3(a). Furthermore, the color maps of the calculated angle-resolved reflectivity spectra without and with taking the resonant exciton into account are shown in Figs. 3(b) and 3(c), respectively. The theoretically calculated exciton-polariton dispersion curves are in good agreement with the measured results as we assign the parameter related to the oscillator strength to be about 4.5×10^4 meV^2 in our calculations. This value is reasonable for the materials with wide band gap and large oscillator strength.[15,16] In Fig. 3(b), the pure cavity mode, marked with *C*, follows the parabolic dispersion, which is consistent with the Bragg mode from the low energy side of the stop band. However, when we consider the resonant exciton in our calculation, the behavior shown in Fig. 3(c) is the characteristic of mode mixing between the cavity and exciton modes, and the formation of lower and upper polariton branches (LPB and UPB) near the angle of about 34°. Under this circumstance, the photonlike LPB will approach to excitonlike LPB with increasing angle. Therefore, the LPB dispersion curve does not follow the original pure photon parabolic dispersion curve because of the strong interaction between photon and exciton modes. In
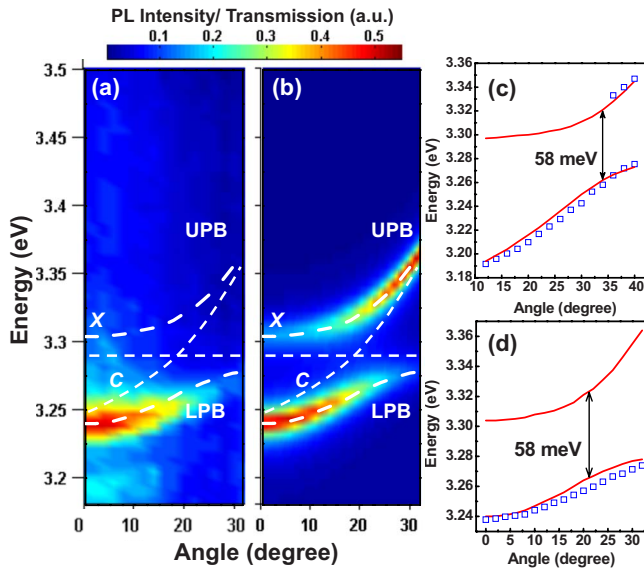
FIG. 4. (Color online) (a) The color map of the measured angle-solved PL spectra from 0° to 32° at RT. (b) The color map of the calculated angle-solved transmission spectra from 0° to 32° with taking the resonant exciton into account. Measured (empty squares) and calculated (solid lines) dispersion curves as the cavity and exciton modes are resonant at (c) 34° and (d) 21°.

the color map of the measured angle-resolved reflectivity spectra shown in Fig. 3(a), the dispersion of the LPB deviates from the parabolic cavity mode and approach to exciton mode with increasing angle. Therefore, by comparing Figs. 3(a) and 3(b), the strong coupling phenomenon between exciton and photon modes is observed in this hybrid ZnO-based microcavity structure. Although the signature of the UPB is not obvious on this color map plotted in linear scale, the broad dip of the UPB could be identified as the measurement angle larger than 35°.

In order to further confirm the strong coupling phenomenon, the measurement of angle-resolved PL is performed at different sample positions, which has relatively small detuning between cavity and exciton modes. The excitation source of the PL measurements is a 266 nm radiation from a frequency tripled Ti:sapphire laser. Figure 4(a) shows the color map of the measured angle-resolved PL spectra. We further calculate the color map of the angle-resolved transmission spectra using the same detuning value, as shown in Fig. 4(b). The calculated LPB is also in good agreement with the measured results. In Fig. 4(a), the signature of the UPB is not obvious on the measured angle-resolved PL map, which is a common feature of wide band gap MC.[12] It should be noted that clear observation of the LPB is more important for the investigation of Bose–Einstein condensation and polariton lasing.[13]

For clearly comparing the theoretical and experimental exciton-polariton dispersion curves with two different cavity-exciton detuning values, we further summarize the results shown in Figs. 3(a) and 4(a), and then illustrate in Figs. 4(c) and 4(d). The empty squares in Figs. 4(c) and 4(d) represent the experimental reflectivity dip and PL emission peak values, respectively, and the solid lines represent calculated results. By comparing Figs. 4(c) and 4(d), the different

exciton-polariton dispersion curves due to different detuning values can be obviously observed. The identical vacuum Rabi splitting value of about 58 meV is estimated at the resonant angle of 34° and 21°, respectively, due to the two different detuning values. This vacuum Rabi splitting value is larger than the previous report,[13] which may originate from the improvement of reflectivity of bottom DBR, higher cavity quality value, and larger ZnO thickness.

In summary, the strong exciton-photon coupling at RT has been observed from the ZnO-based hybrid microcavity structure. The dispersion curves based on angle-resolved reflectivity and PL measurements show obvious characteristics of strong exciton-photon coupling. Theoretically calculated exciton-polariton dispersion curves are in good agreement with the measured results. The large vacuum Rabi splitting value of about 58 meV is estimated from both different cavity-exciton detuning values. These results reveal that ZnO-based microcavities are promising candidate for the realization of microcavity polariton devices.

[1] C. Weisbuch, M. Nishioka, A. Ishikawa, and Y. Arakawa, Phys. Rev. Lett. **69**, 3314 (1992).
[2] R. Butté, G. Christmann, E. Feltin, J.-F. Carlin, M. Mosca, M. Ilegems, and N. Grandjean, Phys. Rev. B **73**, 033315 (2006).
[3] G. Christmann, R. Butté, E. Feltin, J.-F. Carlin, and N. Grandjean, Phys. Rev. B **73**, 153305 (2006).
[4] K. J. Vahala, Nature (London) **424**, 839 (2003).
[5] H. Deng, G. Weihs, C. Santori, J. Bloch, and J. Yamamoto, Science **298**, 199 (2002).
[6] S. Christopoulos, G. Baldassarri Höger von Högersthal, A. Grundy, P. G. Lagoudakis, A. V. Kavokin, J. J. Baumberg, G. Christmann, R. Butté, E. Feltin, J.-F. Carlin, and N. Grandjean, Phys. Rev. Lett. **98**, 126405 (2007).
[7] G. Christmann, R. Butté, E. Feltin, J.-F. Carlin, and N. Grandjean, Appl. Phys. Lett. **93**, 051102 (2008).
[8] S. I. Tsintzos, N. T. Pelekanos, G. Konstantinidis, Z. Hatzopoulos, and P. G. Savvidis, Nature (London) **453**, 372 (2008).
[9] M. Saba, C. Ciuti, J. Bloch, V. Thierry-Mieg, R. André, L. S. Dang, S. Kundermann, A. Mura, G. Bongiovanni, J. L. Staehli, and B. Beveaud, Nature (London) **414**, 731 (2001).
[10] M. Zamfirescu, A. Kavokin, B. Gil, G. Malpuech, and M. Kaliteevski, Phys. Rev. B **65**, 161205 (2002).
[11] K. Kornitzer, T. Ebner, K. Thonke, R. Sauer, C. Kirchner, V. Schwegler, M. Kamp, M. Leszczynski, I. Grzegory, and S. Porowski, Phys. Rev. B **60**, 1471 (1999).
[12] G. Christmann, R. Butté, E. Feltin, A. Mouti, P. A. Stadelmann, A. Castiglia, J.-F. Carlin, and N. Grandjean, Phys. Rev. B **77**, 085310 (2008).
[13] R. Shimada, J. Xie, V. Avrutin, Ü. Özgür, and H. Morkoç, Appl. Phys. Lett. **92**, 011127 (2008).
[14] G. S. Huang, T. C. Lu, H. H. Yao, H. C. Kuo, S. C. Wang, C.-W. Lin, and L. Chang, Appl. Phys. Lett. **88**, 061904 (2006).
[15] N. Ollier, F. Natali, D. Byrne, P. Disseix, M. Mihailovic, A. Vasson, J. Leymarie, F. Semond, and J. Massies, Jpn. J. Appl. Phys., Part 1 **44**, 4902 (2005).
[16] N. Antoine-Vincent, F. Natali, D. Byrne, A. Vasson, P. Disseix, J. Leymarie, M. Leroux, F. Semond, and J. Massies, Phys. Rev. B **68**, 153313 (2003).